Oxygen Production Using Dense Ceramic Hollow Fiber Membrane Modules with Different Operating Modes

Xiaoyao Tan and K. Li
Dept. of Chemical Engineering, Imperial College London, University of London, South Kensington, London SW7 2AZ, U.K

DOI 10.1002/aic.11116
Published online February 16, 2007 in Wiley InterScience (www.interscience.wiley.com).

Oxygen production with three operating modes, i.e. high-pressure operation, sweep-gas operation, and vacuum operation, using dense $La_{0.6}Sr_{0.4}Co_{0.2}Fe_{0.8}O_{3-\alpha}$ (LSCF) hollow fiber membrane modules has been investigated both theoretically and experimentally. The results indicate that the vacuum operation is the best and the most economical operating mode to produce oxygen from air. The sweep-gas operation using water vapor is another choice to obtain a high capacity of oxygen production, providing that problems associated with high temperature sealing can be solved. The high-pressure operation failed to achieve the expected oxygen production capacity. For the LSCF hollow fiber membranes, the surface exchange reaction at the downstream side plays a key role in the oxygen production at operating temperatures lower than 900°C
 AIChE J, 53: 838–845, 2007
Keywords: oxygen production, mixed conducting ceramics, hollow fiber, perovskite membrane

Introduction

Oxygen production is an important process in chemical industries. Currently, it is mainly achieved by cryogenic distillation or by pressure swing adsorption. These methods are costly especially at small and intermediate capacities.[1] Alternately, membrane processes with dense ceramic membranes such as $La_{1-x}Sr_xCo_{1-y}Fe_yO_{3-\alpha}$ (LSCF), which conducts both oxygen ion and electron simultaneously, are more promising in terms of economical production and purity of oxygen.[2–4] When air is applied to one side of the membrane, oxygen can be uniquely transferred through the membrane so long as the gradient of oxygen chemical potential is maintained across the membrane at high temperatures (usually above 700°C). Since only oxygen can be transferred through crystal defects of the ceramic membrane, the downstream gas is of pure oxygen and can be conveniently collected with no further separation processes required.

Correspondence concerning this article should be addressed to K. Li at Kang.Li@Imperial.ac.uk.

However, in order to put this process into commercial applications, there are still many challenges that need to be overcome. For example, the oxygen permeability of the membrane must be improved to a commercially viable value. This depends not only on the membrane material but also on the membrane fabrication. Some progresses have been achieved recently in this field. For instance, a phase inversion/sintering technique was developed for production of ceramic hollow fiber (HF) membranes[5–8] that provide much higher surface area per unit volume when compared with the flat sheet membranes. In addition, since the HF membrane prepared using the phase inversion technique possesses an asymmetric structure, i.e. a thin dense separation layer integrated with the porous substrate of the same material, the resistance to oxygen permeation either due to the bulk diffusion, which relates to the effective membrane thickness (the dense layer), or due to the surface exchange reactions, which depend on the effective surface area, can be greatly reduced, leading to an improved oxygen permeation rate.[9] As a result, a higher oxygen permeation rate can be expected at lower operating temperatures, and hence the lower operating cost. Another challenge to the application of the process is the design of oxygen production systems. The HF membranes can endure higher pressure

difference than can the flat sheet membranes by introducing the feed gas to the outer surface of the fiber. Furthermore, this configuration makes the high temperature sealing less problematic for assembly of membrane modules.

There are three ways to form an oxygen partial pressure gradient across the membranes, which is essential to perform oxygen separation from air: (1) imposing a high pressure on the upstream side (>5 atm) (high-pressure operating mode); (2) applying a vacuum to the downstream side (pressure < 0.2 atm) (vacuum operating mode); and (3) passing a sweep gas through the downstream side (sweep-gas operating mode). For the high-pressure operation, pure oxygen is "pushed out" from air and easily collected in the downstream. However, it requires that the membrane system should be capable of enduring very high pressures at high temperatures, which is hard to achieve for many common materials. The vacuum operation can also produce pure oxygen directly and may provide a higher efficiency than the high-pressure operation,[9,10] although the length of the HFs is limited because of the noticeable pressure drops under the vacuum operation. The sweep-gas operation would not bring the above-mentioned problems, but the downstream gas is a mixture of oxygen and the sweep gas. Accordingly, further separation must be carried out for pure oxygen production. In this context, water vapor is the most feasible candidate among other sweep gases because it is not only abundant but can also be easily separated from oxygen through normal condensation.

In this study, $La_{0.6}Sr_{0.4}Co_{0.2}Fe_{0.8}O_{3-\alpha}$ (LSCF) HF membranes have been prepared by a combined phase inversion/sintering technique. Using the prepared LSCF fibers, three HF membrane modules have been further fabricated and studied for oxygen production with different operating modes both theoretically and experimentally. These results are significant to the design of HF membrane systems for oxygen production.

Modeling of HF modules for oxygen production

Model Formulation. Figure 1 shows a concept of HF membrane module for oxygen production. The air stream flows on the shell side of the module, while the oxygen stream permeated through the HF membranes flows countercurrently in the lumen side. Modeling of the system is based on the LSCF HF membranes with the following assumptions:

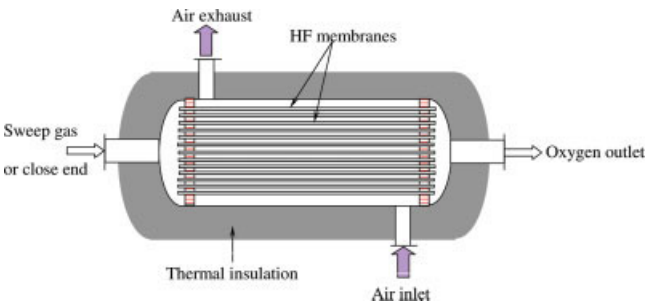

Figure 1. Concept of the hollow fiber membrane module for oxygen production.

[Color figure can be viewed in the online issue, which is available at www.interscience.wiley.com.]

- The mass transfer resistance in the gas phase to oxygen permeation is negligible.
- The oxygen concentration in the upstream (shell side) is constant, while the gas stream in the fiber lumen is plug flow.
- Both the diffusion coefficient of oxygen vacancy and the surface exchange rate constants are independent of oxygen partial pressures. This assumption may not be true for other oxides. However, it has been shown by Xu and Thomson[4] that for $La_{0.6}Sr_{0.4}Co_{0.2}Fe_{0.8}O_{3-\alpha}$ the surface exchange kinetics and the bulk diffusion depend only on the temperature. Therefore, the above assumption is, in general, valid.
- Ideal gas law is applicable to describe the gas behavior of both single component and gas mixture.
- The operation runs isothermally at steady state. This implies that both the air and the water vapor (sweep gas) streams have the same temperature.

Accordingly, the governing equations for the system may be given as follows:

Oxygen conservation equation in the fiber lumen:

$$\frac{d}{dl}\left(\frac{p''_{O_2}V_l}{RT}\right) = 2\pi m R_m J_{O_2} \tag{1}$$

where J_{O_2} is the local oxygen permeation flux expressed by[10]:

$$J_{O_2} = \frac{k_r\left[(p'_{O_2})^{0.5} - (p''_{O_2})^{0.5}\right]}{\frac{R_m}{R_o}(p''_{O_2})^{0.5} + \frac{2k_f(R_o-R_{in})}{D_V}(p'_{O_2}p''_{O_2})^{0.5} + \frac{R_m}{R_{in}}(p'_{O_2})^{0.5}} \tag{2}$$

Water vapor (sweep gas) conservation equation in lumen (the sweep-gas operation):

$$\frac{(p_l - p''_{O_2})V_l}{RT} = F_w \tag{3}$$

The pressure drop in the fiber lumen is described by Hagen-Poiseuille equation:

$$\frac{dp_l}{dl} = -\frac{8\mu V_l}{m\pi R_{in}^4} \tag{4}$$

In the above-mentioned Eqs. 1–4, p_{O_2}' and p_{O_2}'' are the oxygen partial pressures on the outer and the inner surfaces of the HF membranes, respectively, Pa; V_l, the volumetric flow rate of the lumen stream, m^3/s; m, the number of HFs; R_m, the algorithm mean radius, $R_m = (R_o - R_{in})/(\ln(R_o/R_{in}))$, in which R_o and R_{in} are respectively the outer and the inner radius of the HFs, m. F_w is the molar flow rate of water, mol/s; p_l, the pressure in the fiber lumen, Pa; μ, the viscosity of the lumen gas, Pa s; D_V, the diffusion coefficient of oxygen vacancy, m^2/s. k_f and k_r are, respectively, the forward and the reverse reaction rate constants for the surface exchange reactions:

$$\frac{1}{2}O_2 + V_O^{\bullet\bullet} \overset{k_f/k_r}{\longleftrightarrow} O_O^x + 2h^\bullet \tag{5}$$

where the charged defects are defined using the Kröger-Vink notation. That is, O_O^x stands for lattice oxygen, $V_O^{\bullet\bullet}$ for oxygen vacancy, and $h_i^\bullet$ for electron hole.

Table 1. Parameters for the Simulations

Hollow fiber membrane	$La_{0.6}Sr_{0.4}Co_{0.2}Fe_{0.8}O_{3-\alpha}$ (LSCF)	
Number of hollow fiber membranes (m)	500	
Outer diameter (d_o) of the hollow fibers	0.1562 cm	
Inner diameter (d_{in}) of the hollow fibers	0.1125 cm	
Length of the fibers (L)	50 cm	
Membrane area (A_m)*	1.05 m^2	
Air pressure on the shell side (p_s)	1.0 atm	
Oxygen concentration on the shell side (y_s)	0.21	
Operating temperature (T)	950°C	
Pressure at the oxygen outlet (p_o)	1 atm	
Sweep-gas feed flow rate (F_w)	50 cm^3/min	
Diffusion coefficient of oxygen vacancy	$D_V = 1.58 \times 10^{-2} \exp(-8852.5/T)$ cm^2/s	Ref. 4
Forward reaction rate constant of the surface reaction	$k_f = 5.90 \times 10^6 \exp(-27291/T)$, $cm/(atm^{0.5}\ s)$	Ref. 4
Reverse reaction rate constant of the surface reaction	$k_r = 2.07 \times 10^4 \exp(-29023/T)$, $mol/(cm^2\ s)$	Ref. 4

*Membrane area, $A_m = 2\ \pi R_m\ Lm$

The boundary conditions are given by

$$l = 0, \quad p''_{O_2} = 0; \qquad l = L, \quad p_l = p_o \tag{6}$$

where p_o is the pressure at the outlet of the module.

As can be seen, the governing equations for each operating mode are a group of ordinary differential equations, and thus can be solved numerically using the Runge-Kutta method.

Comparison of the Three Operating Modes. The simulation study aims at a pilot oxygen production system with a capacity of about 3 l O_2/min using a HF module containing LSCF HF membranes. Values of the parameters listed in Table 1 are employed for the simulations unless otherwise specified.

Figure 2 shows the oxygen production rate as a function of the water (used as the sweep-gas mode) flow rate. As expected, the oxygen production rate increases as the water rate is increased because the oxygen concentration in the lumen side is decreased, giving the increased driving force for the oxygen permeation. When the water flow rate is at 25 cm^3/min, the oxygen production rate can be reached to 3.1 l/min. At the water flow rate of 150 cm^3/min, the oxygen production rate is achieved as high as 5.4 l/min. The effect of pressure drop in the HF lumen is studied and the result is also plotted in Figure 2. It can be seen that although the pressure drop in the fiber lumen increases almost linearly with the water flow rate because of the introduction of water vapor in the fiber lumen, the pressure drop in the fiber lumen is small. For example, it only gives rise to a pressure drop of 0.04 atm when the water flow rate is at 150 cm^3/min, i.e., only 5% of the operating pressure. Accordingly, the effect of pressure drop on oxygen production is considered to be negligible in the mode of the sweep-gas operation.

Figure 3 illustrates the oxygen production rates versus upstream pressures for the high-pressure operation. As can be seen, the oxygen production rate increases as the operating pressure at the upstream is increased. However, the oxygen production rate is very low and is only at 1.62 l/min (much less than 3 l/min) even when the upstream operating pressure is increased to 50 atm. The reason for this low production is due to the resistance to oxygen permeation, which also increases as the upstream pressure is increased as shown in Eq. 2. Similar to the sweep-gas operation, the pressure drop in fiber lumen is very small and can be neglected in the high-pressure operation as illustrated in Figure 3.

Figure 4 depicts the oxygen production for the vacuum operating mode. It can be seen that the higher vacuum level results in an increase in the oxygen production. The calculation

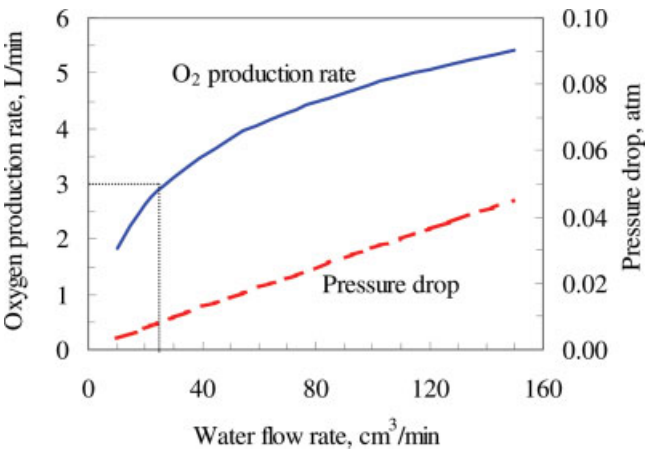

Figure 2. Oxygen production rate as a function of water flow rate.

[Color figure can be viewed in the online issue, which is available at www.interscience.wiley.com.]

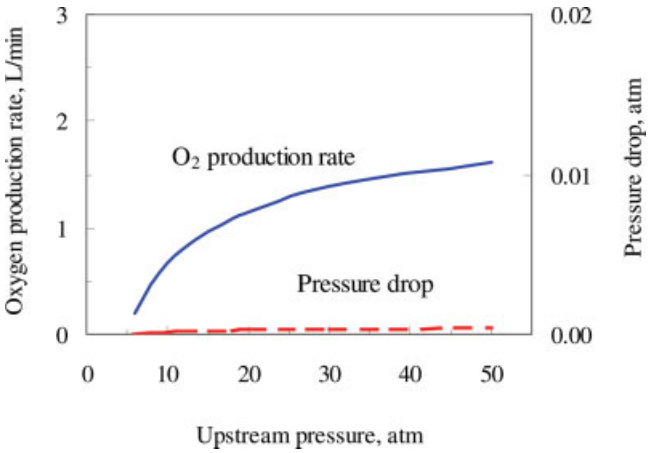

Figure 3. Effect of upstream pressure on the oxygen production by high-pressure operation.

[Color figure can be viewed in the online issue, which is available at www.interscience.wiley.com.]

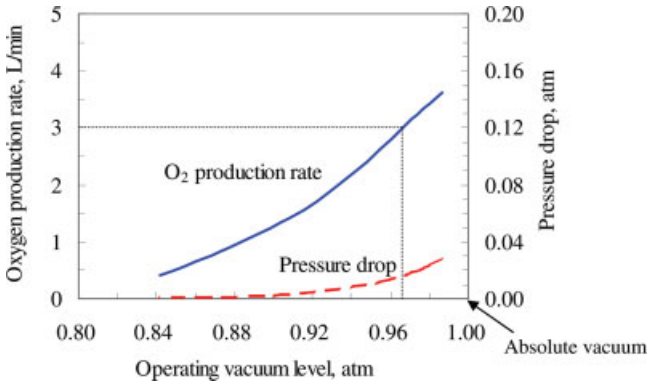

Figure 4. Effect of vacuum level on the oxygen production by vacuum operation.

[Color figure can be viewed in the online issue, which is available at www.interscience.wiley.com.]

results indicate the required oxygen production rate, i.e., 3 l/min can be easily achieved using the same HF module by means of the vacuum operation as long as the vacuum level is at 0.965 atm, at which the absolute pressure is 26.6 mm Hg. The effect of operating vacuum level on the pressure drop in the fiber lumen is also plotted in Figure 4. As can be seen, the pressure drop in the fiber lumen increases as the vacuum level is increased and it becomes very noticeable with respect to the vacuum level, especially at the high vacuum level. This implies that very high vacuum level may lead to a decrease in efficiency, especially for the small and long HF membranes.

In addition to the oxygen production capacity, energy consumption is another important factor that has to be taken into the consideration. On the basis of the two reports given by Air products[11] and Praxair,[12] the ceramic membrane process is able to save at least 30% cost over traditional processes such as pressure swing adsorption, vacuum swing adsorption, or cryogenic distillation. Therefore, in this study, comparison of energy consumption is only carried out between the sweep-gas and vacuum operating modes.

Basically, the energy consumption for these two operating modes includes two parts: (1) the power to heat up the feed air and (2) the power to produce water vapor (sweep gas operation) or the power to pull out the oxygen from the membrane system (vacuum operation). For the two different operating modes, the power required for heating up the feed air is identical and can be excluded in the comparison. Therefore, in Table 2, only the power required for the sweep-gas operation (to produce water vapor) and for the vacuum operation is listed for oxygen production capacity of 3 l/min. It can be seen that the vacuum operation requires much less energy when compared with the sweep-gas operation wherein huge energy to evaporate water into a "sweep-gas" is required. The power required to pull 3 l/min of O_2 out of the HF membrane module is only about 5.06 W, which is much less than that required for sweep-gas operation (1745 W). Nevertheless, it should be realized that the unit cost for heating energy is cheaper than that for the vacuum pump. Also, a part of the energy in the high temperature exhaust gas/vapor stream can be recovered. In addition, the sweep-gas operation is also capable of providing much larger production capacity when compared with the vacuum operation if more sweep gas (i.e., energy) is given.

Table 2. Power Comparison for the Production Capacity of 3 l/min of O_2

	Power Required (W)	
Basis for Calculation	Water Vapor as Sweep-Gas	Vacuum Operation
To evaporate 25 ml water/min and then heat to the required temperature	1745	–
To pull oxygen out of the module	–	5.06

It should be noted that the power to pump water and air into the module is small and is negligible when compared with that used in heating.

In summary, with the HF membrane module containing 500 LSCF hollow fibers (OD/ID of the fiber: 0.156/0.112 cm and $L = 50$ cm, giving the effective membrane area of about 1.05 m^2), the oxygen production rate of 3 l/min can be achieved either by the sweep-gas operation or by the vacuum operation, but failed to be achieved by the high-pressure operation. The total cross-sectional area of these fibers is around 9.55 cm^2. If they are integrated into a bundle with an interstice fraction of 40%, the diameter of the fiber bundle is only 5.5 cm.

Experimental

Materials

Commercially available $La_{0.6}Sr_{0.4}Co_{0.2}Fe_{0.8}O_{3-\alpha}$ (LSCF) powders with the surface area of 9.53 m^2/g and $d_{50} = 0.6$ μm [purchased from Praxair Surface Technologies, USA] were used as the membrane material. Polyethersulfone [(Radel A-300), Ameco Performance, USA] and *N*-methyl-2-pyrrolidone (NMP) [synthesis grade, Merck] were used as the polymer binder and the solvent, respectively. Poly(vinylpyrrolidone) (K30) [from Fluka, $M_w = 40{,}000$] was used as the additive and also to regulate the viscosity of the starting suspension. A surfactant, Arlacel P-135 was used as the dispersant. The mixture of 50 wt % NMP and deionized water was used as the bore liquid while tap water was used as the external coagulant.

Preparation of the LSCF HF membranes

LSCF HF membranes were prepared by a combined phase-inversion/sintering technique described in detail elsewhere.[5] The parameters employed for preparing the LSCF HF membranes in this work are summarized in Table 3. The sintering

Table 3. Parameters for Preparing LSCF Hollow Fiber Membranes

Starting suspension composition, wt %	Values
LSCF powder	66.27
PESf	6.63
NMP	26.51
PVP	0.50
Dispersant	0.09
Dope temperature, °C	20
Internal coagulant composition	50% NMP-water solution
Injection rate of internal coagulant, ml/min	9.0
Nitrogen pressure, atm	1.0
Air gap, cm	0.0
Sintering temperature, °C	1300
Sintering time, h	3

Table 4. Properties of the Membrane Modules for Oxygen Production

	Module A	Module B	Module C
Operating mode	Vacuum	Vacuum	Sweep-Gas
OD of the hollow fiber, cm	0.146	0.146	0.146
ID of the hollow fiber, cm	0.114	0.114	0.114
Number of the hollow fibers	10	22	6
Length of the hollow fiber, cm	24	24	26
Fiber length at constant temperature zone of the furnace, cm	6	6	4
Effective membrane area, cm^2	24.37	53.61	9.75
CARBOLITE furnace type	MTF 12/38/250	MTF 12/38/250	MTF 10/25/130
Maximum temperature, °C	1200	1200	1000

temperature of 1300°C and time of 3 h were proved to be high and long enough to make the membrane gas-tight.

Oxygen production using the LSCF HF membrane modules

Three HF membrane modules were fabricated for oxygen production experiments. Table 4 summarizes the properties of the membrane modules prepared. Modules A and B were developed for the vacuum operation. Thus, HFs used are all "test tube" type with the open end side glued onto a glass holder for suction. Module C consists of 6 fibers with both the ends open for the sweep gas operation. All the HFs were individually tested to be gas-tight before the module fabrication using a gas permeation apparatus developed by Tan et al.[9]

The experimental apparatuses for oxygen production are illustrated in Figure 5. In Figure 5A, a self-cleaning dry vacuum system (model 2025, from Welch) was connected to the fiber lumen of the module at the open end. Most part of the HFs from the closed end was located in the CARBOLITE furnace (MTF 12/38/250) tube. The temperature profile within the furnace tube was measured in advance of experiments using the Type C thermocouple with a thermometer supplied by Omega Engineering Inc. The flow rate of the oxygen pulled out of the membrane module by the vacuum pump was measured using a soap bubble meter. Because of the slight leakage of the vacuum pump, the product gas from the vacuum pump is not of pure oxygen, but over 60%. Therefore, an oxygen analyzer (572, Servomex) was used to measure the oxygen concentration in the stream in order to check the mass balance of permeated oxygen.

For the sweep-gas operation as shown in Figure 5B, a smaller CARBOLITE tubular furnace (MTF 10/25/130) was applied so that the sealing joints of module can be kept far from the inlet of the furnace tube. Furthermore, it is difficult to obtain a constant flow of water vapor because of the restriction of the apparatus. Therefore, argon was used as the sweep gas instead of water vapor to study the performances of the HF membrane module under the sweep-gas mode. The flow rates of argon were controlled and measured using a mass flow controller (Smart Mass Flow meter with Read out & Control Electronics, model 0152, Brooks Instrument). Obviously, the oxygen permeation rate may be calculated directly by multiplying the flow rate of the product stream with the oxygen concentration since no oxygen is present in the sweep-gas inlet.

Results and Discussion

Membrane structure

Figure 6 shows the Scanning Electron micrographs of the prepared LSCF HF membranes. It can be seen that the HF membrane has an asymmetric structure and is composed of finger-like structures beneath the outer surface of the fiber wall. This structure was achieved by using a mixture of 50% NMP aqueous solution as the internal coagulant and is different from the previously prepared fibers wherein finger-like structures beneath both the inner and outer surfaces were achieved using pure water as the internal coagulant.[5] The prime reason to eliminate the inner finger-like structure is to enhance the fiber mechanical strength. Although the elimination of the inner finger-like structure does not favor the oxygen permeation at lower temperatures (<850°C), it shows no effect for the oxygen permeation at higher temperatures (>950°C).[9] With the sintering temperature controlled at 1300°C, it was found that 3 hours is long enough to make the LSCF HF membranes to be gas-tight.

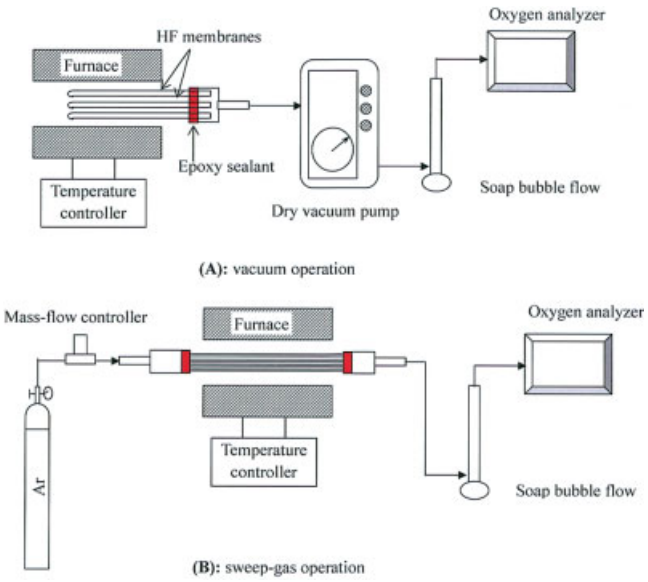

Figure 5. Experimental setup: (A) vacuum operation; (B) sweep-gas operation.

[Color figure can be viewed in the online issue, which is available at www.interscience.wiley.com.]

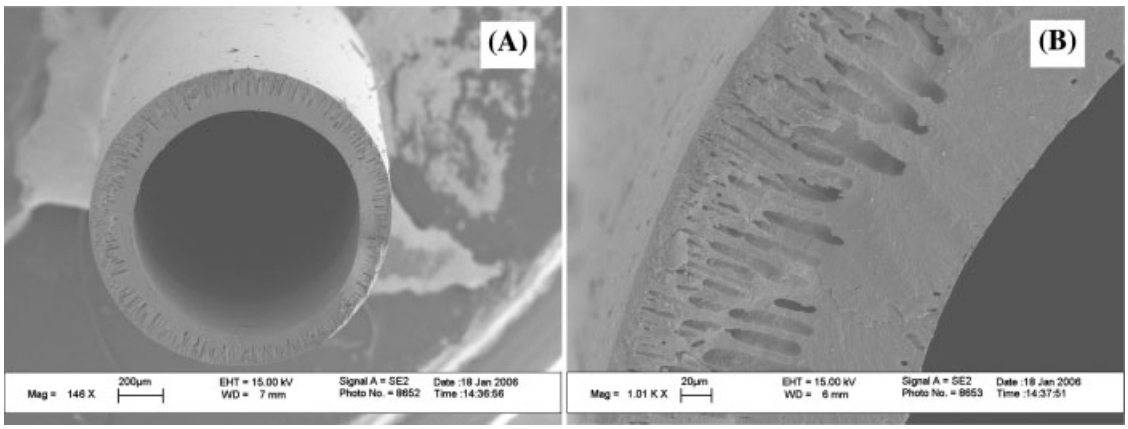

Figure 6. Scanning electron photomicrographs of the prepared LSCF hollow fiber membrane: (A) cross section; (B) membrane wall.

Vacuum operation

Figure 7A shows the experimental results of oxygen production with Module A by applying a vacuum level of 100.6 kPa. As can be seen, at temperatures lower than 500°C, no oxygen permeation takes place, as the data show that the oxygen concentration in the product stream is 21% and flow rate of the stream is 119 cm^3/min because of the leakage of the vacuum pump. After the temperature is increased to above 780°C, oxygen permeation takes place. Both the oxygen concentration and the total product flow rate increase as temperature is increased because the oxygen permeation rate increases with increase of operating temperature. At the operating temperature of 1180°C, the flow rate in the product stream reaches 270.5 cm^3/min, giving the corresponding pure oxygen production rate of 270.5 − 119 = 151.5 cm^3/min if the membrane is gas-tight. Figure 7B compares the measured oxygen concentrations in the product stream to those calculated ones. It can be seen that they are in excellent agreement, further confirming that the leakage is only due to the vacuum pump and the membrane used for the experiments is gas-tight.

Comparison between the experimental data and theoretical results is given in Figure 8, where the oxygen permeation fluxes obtained from different modules at different vacuum levels are plotted against operating temperatures. It can be seen that the experimental data are in good agreement with the theoretical curves with exception that at higher temperatures, the experimental data is slightly inferior to the

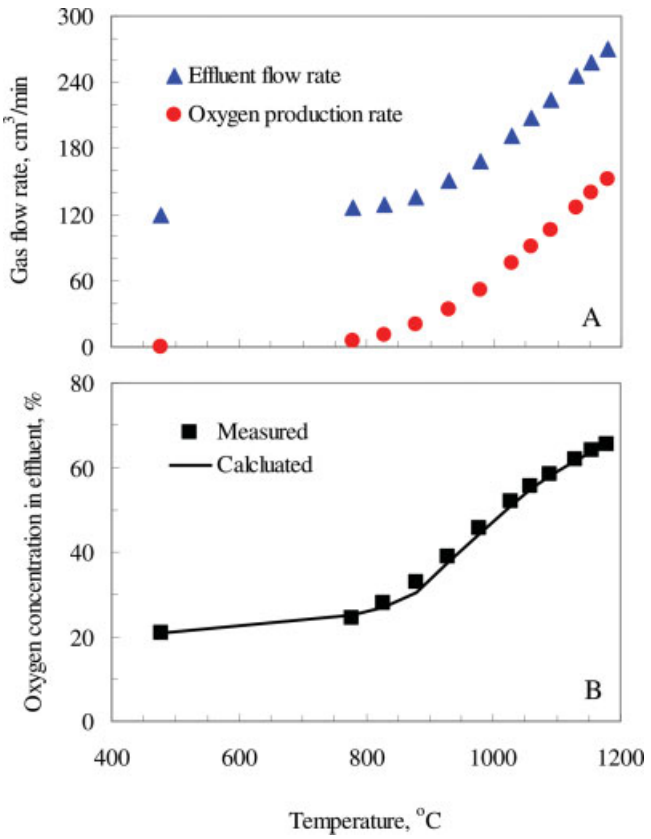

Figure 7. Experimental result of the vacuum operation (Module A, vacuum level = 100.6 kPa).

[Color figure can be viewed in the online issue, which is available at www.interscience.wiley.com.]

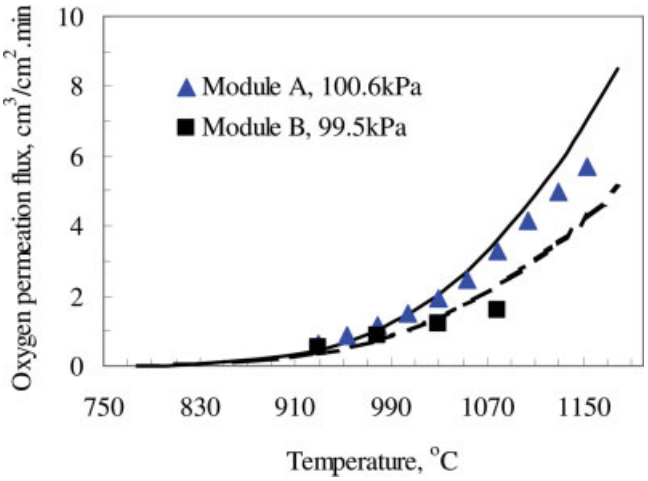

Figure 8. Comparison between experimental data and theoretical results (vacuum operation).

[Color figure can be viewed in the online issue, which is available at www.interscience.wiley.com.]

simulation results. This is probably due to the lower oxygen concentration in the tubular furnace (oxygen concentration in feed side). Since the HF membranes are located horizontally in centre part of the furnace tube, the hot air in the furnace is the only feed source. At higher temperatures, because of the high oxygen permeation flux, the permeated oxygen from the furnace cannot be compensated in time by air outside of the furnace, leading to lower oxygen concentration of air in the furnace, hence giving the slight difference between experimental and theoretical results.

Figure 9 shows the experimental results of different operating cycles of the Module A with the vacuum level of 100.6 kPa. One operating cycle means a whole operating process, i.e. heating up the module from room temperature, collecting experimental data at high temperatures, and cooling the module back to the ambient temperature. It can be seen that the oxygen production rates in Cycle 1 are lower than those in Cycle 2 and Cycle 3, especially at lower temperatures. However, as the temperature is increased to 1078°C, the difference in oxygen production rates between Cycle 1 and the other cycles is diminished. Afterwards, the oxygen production rates in the Cycle 2 and Cycle 3 are almost identical, suggesting the membrane is relatively stable between the cycles.

Sweep-gas operation

Figure 10 shows the experimental results of the sweep-gas operation using Module C. It can be seen that the oxygen concentration in the permeate stream decreases with increasing the argon flow rate for all the operating temperatures. Figure 10 also shows that experimental data are lower than the theoretical results at lower operating temperatures. This certainly resulted from the membrane structure designed. As mentioned earlier, the inner finger-like structure was eliminated for the enhancement of fiber mechanical strength in this study. This results in a reduction of inner surface area for the surface exchange reactions, hence considerable increase in oxygen permeation resistance, especially at lower operating temperatures.[9] The above results further strengthen the conclusion in our earlier study[9] that the surface exchange reaction at the downstream side of the membrane plays a key role in the oxygen permeation at operating temperatures lower than 900°C.

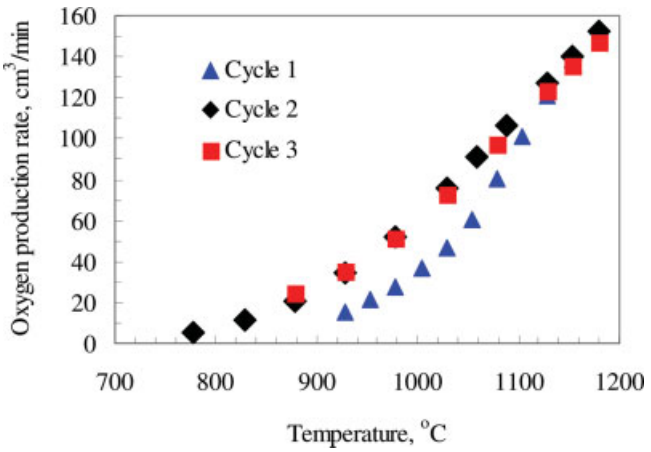

Figure 9. Experimental results for the different operating cycles (Module A, vacuum level = 100.6 kPa).

[Color figure can be viewed in the online issue, which is available at www.interscience.wiley.com.]

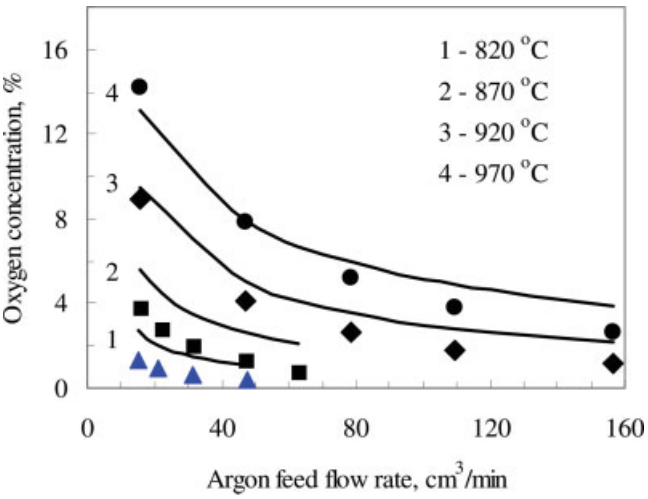

Figure 10. Experimental and theoretical results for the sweep-gas operation (Module C).

[Color figure can be viewed in the online issue, which is available at www.interscience.wiley.com.]

It should be noted that when water vapor is used as a sweep gas in studying the performances of the HF membrane module under the sweep gas condition, the operating performance is expected to be identical. However, stability of the membrane and the membrane module would be the main issue, which we are currently unable to address because of the restriction of experimental apparatus. It is anticipated that this issue will be fully investigated when the appropriate experimental apparatus becomes available.

Conclusions

Dense asymmetric LSCF HF membranes have been prepared using an immersion induced phase inversion followed by sintering at 1300°C for 3 h. Oxygen production using the prepared LSCF HF membranes has been investigated both theoretically and experimentally. The vacuum operation is the best choice for oxygen production from air in terms of the production cost. The sweep-gas operation with water is another choice if the problems associated with high temperature sealing can be overcome. The surface exchange reaction at the downstream side of the membrane plays a key role in the oxygen permeation at operating temperatures lower than 900°C.

Acknowledgments

The authors gratefully acknowledge the research funding provided by EPSRC in the United Kingdom (grant no. GR/S12203).

Notation

A_m = Membrane area, $A_m = \frac{2\pi(R_o - R_{in})L}{\ln(R_o/R_{in})}$, m^2
D_V = Effective diffusivity of oxygen vacancy, m^2/s
F_w = Sweep-gas feed flow rate, mol/s
k_r = Reverse surface reaction rate constant of Eq. 5, mol/(m^2 s)
k_f = Forward surface reaction rate constant of Eq. 5, m/($Pa^{0.5}$ s)

l = Length variable of hollow fiber membrane, m
L = Length of hollow fiber membrane, m
m = Number of hollow fiber membranes
p_l = Pressure in the fiber lumen, Pa
p_o = Pressure at the outlet of the HF module, Pa
p'_{O_2}, p''_{O_2} = Oxygen partial pressures in the upstream and the downstream, Pa
R = Gas constant, 8.314 J/(mol K)
R_{in}, R_o = Inner and outer radius of hollow fiber, m
R_m = Algorithm mean radius of hollow fiber, $R_m = \frac{R_o - R_{in}}{\ln(R_o/R_{in})}$
T = Operating temperature, K
V_l = Volumetric flow rate of the lumen gas stream, m^3/s
μ = gas viscosity, Pa s

Literature Cited

1. Luyten J, Buekenhoudt A, Adriansens W, Cooymans J, Weyten H, Servaes F, Leysen R. Preparation of $LaSrCoFeO_{3-x}$ membranes. *Solid State Ionics*. 2000;135:637–642.
2. Li S, Jin W, Xu N, Shi J. Synthesis and oxygen permeation properties of $La_{0.2}Sr_{0.8}Co_{0.8}Fe_{0.2}O_{3-\delta}$ membranes. *Solid State Ionics*. 1999;124:161–170.
3. Stefan D, Herle JV. Oxygen transport through dense $La_{0.6}Sr_{0.4}Fe_{0.8}$-$Co_{0.2}O_{3-\delta}$ perovskite-type permeation membranes. *J Eur Ceram Soc*. 2004;24:1319–1323.
4. Xu SJ, Thomson WJ. Oxygen permeation rates through ion-conducting perovskite membranes. *Chem Eng Sci*. 1999;54:3839–3850.
5. Tan X, Liu Y, Li K. Preparation of $La_{0.6}Sr_{0.4}Co_{0.2}Fe_{0.8}O_{3-\alpha}$ hollow fibre membranes for oxygen production by a phase-inversion/sintering technique. *Ind Eng Chem Res*. 2005;44:61–66.
6. Li K, Tan X, Liu Y. Single-step fabrication of ceramic hollow fibres for oxygen permeation. *J Membr Sci*. 2006;272(1/2):1–5.
7. Liu S, Gavalas G. Oxygen selective ceramic hollow fibre membranes. *J Membr Sci*. 2005;246(1):103–108.
8. Schiestel T, Kilgus M, Peter S, Caspary KJ, Wang H, Caro J. Hollow fibre perovskite membranes for oxygen separation. *J Membr Sci*. 2005;258(1/2):1–4.
9. Tan X, Liu Y, Li K. Mixed conducting ceramic hollow fibre membranes for air separation. *AIChE J*. 2005;51:1991–2000.
10. Tan X, Li K. Modeling of air separation in a LSCF hollow-fibre membrane module. *AIChE J*. 2002;48:1469–1477.
11. Air Products and Chemicals, Inc. Cheaper, more efficient oxygen through novel production method. (Research and data for Status Report 3-01-0041, available at http://statusreports.atp.nist.gov/reports/93-01-0041.htm.) ATP Status Report Database Search Results, National Institutes of Standards and Technology.
12. Praxair, Inc. O_2-Selective materials to lower the cost of oxygen. (Research and data for Status Report 94-01-0111, available at http://statusreports.atp.nist.gov/reports/94-01-0111.htm.) ATP Status Report Database Search Results, National Institutes of Standards and Technology.

Manuscript received July 3, 2006, and revision received Dec. 20, 2006.